0 0 0 0 4 0 4 7 6 9 8 7 0

UC-38
LBL-6266
c. 1

KINETICS OF FORMATION OF THE A-15 PHASE IN THE Nb-Al-Ge SYSTEM

Elijah Kannatey-Asibu, Jr.

(M. S. thesis)

May 1977

LIBRARY AND DOCUMENTS SECTION

Prepared for the U. S. Energy Research and Development Administration under Contract W-7405-ENG-48

For Reference

Not to be taken from this room

LAWRENCE BERKELEY LABORATORY
UNIVERSITY OF CALIFORNIA
BERKELEY

LBL-6266
c. 1

DISCLAIMER

This document was prepared as an account of work sponsored by the United States Government. While this document is believed to contain correct information, neither the United States Government nor any agency thereof, nor the Regents of the University of California, nor any of their employees, makes any warranty, express or implied, or assumes any legal responsibility for the accuracy, completeness, or usefulness of any information, apparatus, product, or process disclosed, or represents that its use would not infringe privately owned rights. Reference herein to any specific commercial product, process, or service by its trade name, trademark, manufacturer, or otherwise, does not necessarily constitute or imply its endorsement, recommendation, or favoring by the United States Government or any agency thereof, or the Regents of the University of California. The views and opinions of authors expressed herein do not necessarily state or reflect those of the United States Government or any agency thereof or the Regents of the University of California.

0 0 0 0 4 7 0 1 6 7 1

LBL - 6266

Kinetics of Formation of the A-15 Phase in the Nb-Al-Ge System

By

Elijah Kannatey-Asibu, Jr.

(M. S. Thesis)

0 0000004074171046647 2

KINETICS OF FORMATION OF THE A-15 PHASE IN THE Nb-Al-Ge SYSTEM

Contents

Abstract i

I. Introduction and Historical Background 1

II. Objectives 4

III. Experimental Studies 7

A. Selection of Approach 7

B. Procedure 7

C. Sample Analysis 9

IV. Results and Discussion 14

A. Growth of the A-15 Phase 14

B. Grain Growth. 16

C. Phase Changes 18

V. Conclusions and Recommendations for Further Work 20

Acknowledgements 23

References 24

Tables 25

Figure Captions 28

Figures 29

0 0000040741710416657 3

LBL - 6266

KINETICS OF FORMATION OF THE A-15 PHASE IN THE Nb-Al-Ge SYSTEM

Elijah Kannatey-Asibu, Jr.

Materials and Molecular Research Division, Lawrence Berkeley Laboratory
and Department of Mechanical Engineering, University of California
Berkeley, California 94720

ABSTRACT

A study has been made of the time and temperature dependence of the growth of the A-15 phase and its grains in the Nb-Al-Ge system. In addition, changes in the microstructure and composition of the A-15 phase have been studied using an EDAX analysis. The data obtained have been plotted and compared with theory. The results have been used to explain the variations in the superconducting properties of this system as observed in earlier work. Consequently, areas for further study towards optimizing the superconducting parameters of this system have been proposed.

0 0 0 0 0 0 4 0 7 4 1 7 1 0 4 1 6 6 7 4

I. INTRODUCTION AND HISTORICAL BACKGROUND

There is always a reason behind whatever one does, and that is why, despite the excellent texts and articles in the literature on the applications of superconductors,[1,2] it is considered relevant in this introduction to present a brief review of the potential uses of superconductors.

The A-15 phase of the Nb-Al-Ge system is a well known material with good superconducting properties. However, much work remains to be done to make possible the use of this compound in practical superconductors. Superconductivity has not as yet made a significant impact on society, but it appears that the time is not too far off. Among the most important probable applications will be AC and DC motors and generators, energy transmission (AC and DC cables), high speed ground transportation (magnetically levitated trains), energy storage, and energy production. The principle behind the high speed transportation is one of generating a repulsive force between moving superconducting train magnets and ordinary metal tracks to suspend the train. This way very high speeds can be attained that would not be possible using conventional wheeled trains. The use of superconductors in AC and DC cables will enable power to be transmitted without losses. Though most of these applications are now in the developmental stages, some are projected to be in commercial use by the 1980's.

Prior to 1967, interest in superconductors had been limited to binary compounds. During this period the highest critical temperature, T_c, obtained was that for Nb_3Sn: 18°K. Since the discovery by Matthias, et al.[3] in 1967 of a ternary Nb-Al-Ge compound with a T_c of 20.05°K,

other superconductors with higher or nearly as high T_c's have been reported (namely, Nb_3Ge: 23.2°K; Nb_3Ga: 20.3°K; Nb_3Al: 18.9°K, and Nb_3-(Al, Ga): 19.0°K).[4-9] The value for the Nb-Al-Ge system has been steadily increased since the initial announcement, the highest so far being 21°K reported by J. Ruzicka.[10] Of these superconductors with high critical temperatures, the Nb-Al-Ge system has the highest known upper critical field of 410 kG at 4.2°K,[11] and this explains the attention that it has received in recent years.

The superconducting phase of the system has the A-15 structure, a unit cell of which is shown in Fig. 1 with the niobium atoms forming orthogonal chains on the faces of a body-centered cubic structure at the $\frac{1}{4}\,0\,\frac{1}{2}$, $\frac{1}{2}\,\frac{1}{4}\,0$, $0\,\frac{1}{2}\,\frac{1}{4}$, $\frac{3}{4}\,0\,\frac{1}{2}$, $\frac{1}{2}\,\frac{3}{4}\,0$, $0\,\frac{1}{2}\,\frac{3}{4}$ positions while the aluminum and germanium atoms are statistically dispersed at the corners and center of the cube.

The development of a commercially viable process to fabricate the Nb-Al-Ge superconductor, like all other superconductors with the A-15 structure, presents formidable problems, the reason, as usual, being due to the brittleness of the A-15 phase. The bronze process, which has been used in producing Nb_3Sn commercially, does not work for this system as a result of the σ-phase which forms in the early stages of the reaction and prevents the formation of the A-15 phase. Attempts have been made to use the Kunzler technique to fabricate it,[12] whereby powders of Nb, Al, and Ge are mixed in the right proportions, sealed in a cupronickel tube, and then cold worked by swaging and rolling, after which the outer cupronickel sheath is removed by etching in nitric acid. The tape is then reacted to form the A-15 phase. This is not a parti-

cularly good method in that quite apart from the fact that the tape so produced is not very flexible, there is little control of the microstructure.[13] Other methods have been tried for producing single filament wires.[14,15]

At the Lawrence Berkeley Laboratory a more promising method of preparing Nb-Al-Ge multifilamentary superconductors, the infiltration technique, is presently in use.[16] In this process, a compacted and sintered Nb rod is infiltrated with an Al-Ge alloy of eutectic composition (see Section IIIB). The infiltrated rod is then clad with tantalum and monel tubing and deformed by form and flat rolling. The deformed rods are then reacted to form the superconducting A-15 phase. Tapes with thickness of 0.04 - 0.015 cm and multifilamentary wires of 0.025 cm diameter have been produced by this process.

II. OBJECTIVES

Recent work done at the Materials and Molecular Research Division of the Lawrence Berkeley Laboratory on multifilamentary wires and tapes of the Nb-Al-Ge superconducting system prepared by the infiltration method has shown that the critical temperature, T_c, increases as the reaction temperature is increased.[16] Unfortunately though, the LBL group also found that the critical current density, J_c, decreases in that order, that is, it increases as the temperature is lowered. Furthermore the volume fraction of the superconducting A-15 phase formed at the lower temperatures is much smaller than that formed at the higher temperatures as can be seen from Fig. 2 which shows optical micrographs of samples reacted at 1500°C, 1700°C and 1840°C for 1 and 5 minutes. Consequently, despite the increased critical current density, the overall current-carrying capacity of the superconductor is reduced at the lower temperatures. The reduction in critical current density at the higher temperatures was thought to be due to the lack of pinning centers for the current at those temperatures. When a superconductor is subjected to a magnetic field greater than the lower critical field (H_{c_1}), the field partially enters the superconductor as flux lines which then experience a Lorentz force F_L given by:

$$F_L = J \times B$$

where J is the current density and B is the flux density. The force F_L is per unit volume of superconductor. When the force causes the flux lines to move, they induce an electric field E given by:

$$E = V \times B$$

0 00 00 00 40 74 17 10 41 65 87 6

where V is the velocity of the flux lines. The electric field in turn causes an induced resistance and eventually the superconductor goes normal when the fluxons fully penetrate the conductor, at the upper critical magnetic field, H_{c_2}.

The critical current is the current that causes the flux lines to fully penetrate the conductor at a given magnetic field. Thus it can be seen that if there is nothing pinning the flux lines in position, the superconductor could go normal at a relatively low value of current density. On the other hand, by pinning the fluxoids, as the flux lines are called, high current densities can be sustained since the pinning force then balances the Lorentz force which tends to move them.

Thus it was found necessary to further understand the behavior of the superconducting phase of the Nb-Al-Ge system at those high temperatures with a view to subsequently finding a means to improve the overall superconducting parameters of the system. This project was then undertaken to study how the A-15 phase increases in thickness and how its grain size varies with time and temperature. This would facilitate a determination whether to use grain boundaries as pinning sites or if it would be necessary to find some other means of pinning the flux lines. In addition, the phase thickness studies will give an idea as to how long a time or how high a temperature is necessary for a reasonable current-carrying capacity, given a particular value of J_c. The system under consideration was found to have four phases at the times and temperatures studied by Pickus, et al.[16] What influence the reaction times and temperatures would have on the interactions of these phases was another area that was considered necessary to study.

In summary, the objectives of this work are to study:

1. Grain growth in the A-15 phase.
2. The growth of the A-15 phase itself.
3. The influence of reaction time and temperature on the growth of the other phases.

0 00 00 0 40 74 17 10 41 66 97 7

III. EXPERIMENTAL STUDIES

A. Selection of Approach

The Nb-Al-Ge superconductor can be produced by several methods, some of which have already been discussed and references have been given to a few others (see Section 1). Most of these methods could have been used in the present study, though with varying degrees of difficulty. Due to its simplicity, the infiltration technique was found to be the most appropriate method for the study. A variation of this method which looks even simpler on the surface is the coating method where a solid niobium rod would be dipped into molten Al-Ge eutectic for a reasonable time, pulled out, and shaken to remove excess eutectic adhering to the rod. Samples of the coated rod could then be cut and reacted for examination. Despite the apparent ease of operation, such a method would require several reactions at a given temperature and time in order to give a statistical meaning to the measured parameters.

With the infiltration technique, due to the porous nature of the dipping rod, a given sample affords the opportunity of studying several reacting regions randomly dispersed in the sample as can be seen from Fig. 2, enabling comparisons to be made even within a particular sample. Thus fewer samples need be obtained for the same reacting conditions, reducing the required time and effort.

B. Procedure

Porous niobium rods about 2 1/2 inches in length and 1/8 inch in diameter were prepared as outlined by K. Hemachalam and M. R. Pickus by isostatically pressing niobium powder (-270 + 400 mesh) of 99.9% purity at a pressure of 30,000 psi. This pressure has been found to give ade-

quate porosity and green strength for subsequent infiltration. Each rod was then attached to a tantalum rod using an 0.01 inch tantalum wire and then suspended in the center of the heating element (made of tungsten wire) of an Abar furnace. Fig. 3 shows a cross-section of the set-up, including the Abar furnace. The rod was then sintered at a temperature of 2200°C for 15 minutes under a vacuum of less than 10^{-5}mm Hg.

The aluminum-germanium eutectic was prepared by arc-melting an aluminum (99.999% pure) and germanium (99.999% pure) mixture of the eutectic composition (ie. 53 parts by weight Ge, to 47 parts by weight Al) under an argon atmosphere in a copper-chill mold. The buttons so prepared were cooled, overturned and remelted to ensure proper mixing of the components. They were then cleaned by polishing off the outer layers and melted together in a quartz tube in the Abar furnace under a helium atmosphere. This was repeated several times with the eutectic being placed upside down each time to ensure that all lighter and heavier impurities had been cleaned off. Fig. 4 shows a photomicrograph of the eutectic microstructure and the two components are seen to be in the right proportions, indicating that the 53:47 weight ratio is the appropriate one for the eutectic composition.

Before the Nb rod was sintered, however, the cleaned eutectic was placed below the Abar furnace in the arrangement shown in Fig. 3. A graphite crucible was used for quick and uniform transfer of heat from the heating element to the eutectic.

As the sintered rod was allowed to cool, the eutectic was heated to 600°C (its melting temperature is 424°C). With the eutectic melted and at 600°C and the rod also at about 600°C, the latter was lowered

till it was completely immersed in the molten eutectic. The two were kept at about the same temperature to prevent freezing of the eutectic in the outer pores of the rod and preventing further infiltration. The furnace was then back-filled with helium to a pressure just below atmospheric. This creates a pressure gradient between the surface of the eutectic and the pores in the rod, forcing the eutectic to enter and completely fill the pores. The rod was kept immersed in the melt for 5 minutes to ensure adequate infiltration before being pulled up and allowed to cool to room temperature. A cross-section of an infiltrated specimen is shown in Fig. 5. Each infiltrated rod was then cut into pieces of about 3/16" length, the ends ground to clean off any foreign material that might have been transferred from the cutting saw, and reacted.

In reacting, each specimen was suspended from a tantalum rod as described above, but this time the specimen was shielded from the heating element while the furnace was heated to the required temperature. Before heating, the furnace was evacuated to a pressure less than 10^{-5} mm Hg and afterwards back-filled with helium to prevent excessive evaporation of aluminum during reaction at the high temperatures. Under steady state conditions, the sample was lowered to the heating zone for the required time and then raised back and again shielded from the heat while it cooled.

C. Sample Analysis

Reacted samples were mounted in Kold Mount resin, ground and subsequently polished on a series of Buehler grinders, proceeding from the coarsest to the finest. Final polishing was done on a rotating wheel

containing 0.05 micron Gamma Alumina dispersed in distilled water. Etching was done using a solution of sulphuric acid, hydrofluoric acid, and water, mixed in equal proportions and to which a few drops of hydrogen peroxide had been added.

Etching was found to be one of the crucial stages involved in the analysis. For measurement of the A-15 phase thickness, short etching times were found to be necessary since deep (or longer time) etching caused the A-2 solid solution phase (see Section 4) to cast a shadow on the A-15 phase thickness when examined metallographically. In regard to this aspect of the analysis, samples reacted for shorter times at lower temperatures had to be etched much faster than those reacted at higher temperatures for longer times. On the other hand, much longer etching times were found to be necessary to reveal the grain boundaries clearly. The foregoing is just meant to serve as a guideline for etching specimens and no specific times can be outlined here since much depends on the specimen being etched, the etch being used, and how good a polishing has been done. How successfully one does it will depend on experience.

To facilitate phase identification, etched samples were anodized in a Pickleshimer solution (240 ml ethyl alcohol, 140 ml water, 20 ml phosphoric acid, 40 ml lactic acid, 80 gm citric acid, and 80 ml glycerine) at 27 volts for 6 minutes. Under these conditions the various phases were identified by the following colors:

Nb solid solution (A-2 phase)	-	light gray
A-15 phase	-	light blue

0 0 0 0 8 7 1 0 4 2 1 9

Al-rich (σ) phase	-	blue
Ge-rich phase	-	deep blue

Phase identification is covered in more detail in Section 4.

Having anodized a sample, photomicrographs were then taken at several positions over the cross-section. Measurements of the A-15 phase thickness were done using vernier calipers accurate to 0.05 mm. Readings were taken directly from photomicrographs taken at 1000x. Several readings were taken for a given condition of time and temperature and then averaged.

There are several methods for measuring grain sizes and each depends on the materials under consideration and its characteristic features. Among those used for nonferrous metals and alloys are: the ASTM Comparative Method;[18] Jefferies Planimetric Method;[19] and the Linear Intercept Method.[18]

With the ASTM method, a photomicrograph of the specimen at 100x magnification is compared with standard ASTM charts and from the number (N) of the ASTM chart that closely matches the photomicrograph under study, the mean planar grain area (a) of the specimen is calculated as follows:

$$a(100x) = 2^{N-1} \text{ in}^2$$

This is a simple and quick method for measuring grain size but has the danger of being subject to bias.

The Jefferies Planimetric method is applicable only to materials containing equiaxed grains and in this method, a 79.8 mm diameter circle (area = 5000 mm^2) is drawn on the rough side of the focusing screen

so that the center of the circle and that of the rectangular focusing screen almost coincide and the specimen is focused at a standard magnification. The grains intersected by the circumference of the circle are counted as well as those that are completely enclosed by the circle. From these measurements the average grain size can be calculated using a standard magnification factor.[19] This is an accurate method, but not as simple as the previous one.

The third method, the Linear Intercept method, is quite commonly used. It can be used for non-equiaxed grains, is simple, accurate and free from bias. In this case, random lines with a total length of approximately 1000 times the larger grain sizes are drawn on a photomicrograph of the specimen. The mean grain diameter (d) is obtained by dividing the total length of the lines by the product of the number of grain boundaries crossing the lines and the magnification of the photomicrograph. In other words:

$$d = \frac{\text{Total length of lines}}{\text{No. of grain boundaries x magnification}}$$

For other modifications of this method, see Ref. 18.

On close study of the above methods and the specimen under study it was realized that none of them would be suitable for the system being analyzed. As can be seen from Fig. 2 at low temperatures and short reaction times, say 1500°C for 5 minutes, the microstructure of the specimen was such that a fair comparison could not be made between the A-15 grains (the phase forms small circular bands at several portions of the photomicrograph) and the ASTM charts (which completely fill the micrographs). Also an adequate number of lines could not be clearly drawn

on the A-15 phase for these specimens to enable the linear intercept method to be used. Even though it would have been possible to use either of these methods for some of the high temperature - longer time reactions, it was decided that a new method of analysis had to be used that would be applicable to both types of samples.

The approach adopted in this analysis, even though not a standard method, still gives a measure of the grain size variation with time and temperature, which is the objective of this study. Each grain size was measured in two directions normal to each other with vernier calipers and the readings averaged to give the size of that particular grain. Several grains were measured from each sample as well as other samples at the same time and temperature conditions and averaged. The phase thickness and grain size average values obtained are listed in Table II.

The temperature range investigated was selected on the basis of a previous investigation which had shown that critical temperatures obtained for reaction temperatures below 1300°C were not significant compared to those for higher temperatures,[16] and that they actually increase with increasing temperature. 1840°C was the highest temperature selected for investigation since the highest temperature to which the system can be subjected without partial melting is 1870°C, the 30°C difference being used to allow for possible temperature fluctuation.

Phase identification was done on etched but unanodized specimen using a scanning electron microscope equipped with an EDAX (Energy Dispersive Analysis of X-rays).

IV. RESULTS AND DISCUSSION

A. Growth of the A-15 Phase

The growth of the superconducting A-15 phase is shown in Fig. 6a where the phase thickness is plotted against the reaction time. The graphs show a rapid increase in the A-15 phase thickness during the early stages of a reaction, the rate reducing substantially at long reaction times, even though the phase continues to grow. This growth rate is seen to be more rapid at higher reaction temperatures - a result of the higher thermal energy available for diffusion of atoms of the component elements at those temperatures. The growth rates observed could be explained by the fact that the A-15 phase is sandwiched between phases rich in Nb on one side and rich in Al and Ge on the other side, so that as growth proceeds, the diffusion path increases and the rate of growth therefore decreases. The graphs also show that for a given time, a greater phase thickness is obtained for the higher temperatures. In other words, to obtain a specific volume fraction or thickness, longer reacting times will be required for the lower temperatures and at 1300°C or below, the time may be unusually long.

The growth process involved here is a rather complex one since it comprises different processes at various stages of a reaction. At short times or lower temperatures when the A-15 phase is sandwiched between the A-2 phase (Niobium solid solution) and the sigma (σ), Al-rich phase, (Section IVC), the growth process may involve a phase decomposition on the σ-phase side and interfacial reaction on the solid solution side. The transformation process is one of reconstructive growth involving the breaking of the bonds of the σ-phase and its rearrangement to form the

0 0 0 0 0 4 7 0 4 8 1

A-15 phase. Following the bond-breaking stage, the atoms involved then move across the boundary separating the two phases to form the A-15 phase. This is the interfacial reaction. Processes involving interfacial reactions at one stage or another are often interpreted by diffusion data alone due to the high reaction rates and the basic diffusion mechanisms involved. However since this is a ternary system, simplification of the data in Fig. 6a by analyzing on a purely diffusion basis using Fick's Laws would still require a very complex treatment demanding the use of four diffusion coefficients all of which vary with composition.

To simplify the analytical process further, therefore, the data was replotted on a log-log graph as shown in Fig. 6b. The data points were found to be on straight lines for the time range studied indicating a growth law of the form:

$$d = at^n$$

Where d = A-15 phase thickness

a = rate constant

t = reaction time

n = reaction (growth) index

The points were fitted with straight lines using the linear least squares analysis with a degree of fit of the order of $\pm$ 0.96 (Table III) which shows a good straight line relationship between the points. The growth indices obtained from the slopes of the lines vary between 0.34 and 0.44. This indicates a growth rate less than that predicted by the simplified form of Fick's second law which gives a growth index of 0.5. This reduction in growth rate must be due to the involvement of other processes as discussed above.

B. Grain Growth

There is a considerable amount of literature on the kinetics of grain growth in metals. However most of the work done and consequently the theories proposed up to date have been limited to pure metals, dilute alloys, and the effect of solute interaction on grain boundary mobility.[20] The conclusions drawn from the growth data obtained for this system which is ternary and not dilute may be substantially different from those drawn from the existing theories.

A plot of measured grain sizes against reaction times for the various temperatures, isothermal grain growth curves, are shown in Fig. 7a. Unlike the phase growth considered in the previous section in which the A-15 phase shows a tendency for continuous growth, the graphs here show growth processes that tend to level off at long reacting times. This indicates a tendency towards zero growth rate at long reacting times and could be due to a change in the grain boundary structure from one that is highly mobile in the early stages of a reaction to a virtually stagnant one. In addition, the critical grain size (ie. value of grain size at which the curves level off) is found to depend on the reacting temperature, increasing as the temperature is increased. This and the fact that the growth rate in the early stages is much higher for the higher temperatures (steeper curves) can be explained on the basis of the process being a thermally activated one so that there is more thermal energy available at those temperatures, enabling the atoms to move with much greater velocities. It also explains why at lower temperatures, longer reacting times are required to attain the critical grain size. Thus if one wants to obtain a given grain size for a specimen,

it has to be reacted for longer times at lower temperatures than at higher temperatures, and if the required grain size happens to be greater than the critical size at the temperature in question, then it will not be obtained at all.

Another interesting phenomenon that can be observed from the graphs is the change in grain size from 1500°C to 1700°C, a 200°C temperature difference, and that from 1700°C to 1840°C, a difference of 140°C. The change is found to be much greater for the latter than the former, an effect which is more clearly seen from the isochronal curves in Fig. 7b. This is due to an abnormal grain growth, manifesting itself in a steep rise in the isochronal curves at about 1720°C to 1740°C. The temperature at which it starts is slightly higher for the shorter reaction time (5 min.) than for the longer time (15 min.).

On replotting the data in Fig. 7a on a log-log plot, the points were found to be on straight lines for the time range studied, Fig. 7c. This depicts a power growth law of the form:

$G = Kt^n$ Where G = Average Grain Size

K = Rate Constant

t = reaction time

n = growth law index

The straight lines were fitted to the points using the linear least squares analysis with a degree of fit of the order of $\pm$ 0.97, Table III. The growth law indices lie between 0.33 and 0.46, increasing with increasing temperature and this clarifies the earlier assertion that the growth rate increases with increasing temperature.

In an earlier work on grain growth, Simpson, et al.[21] concluded that a growth law index of n = 0.5 is typical of high purity metals as well as dilute alloys. However the results of the present studies have shown that this does not necessarily apply to alloys with the component elements in substantial concentrations. In this case, grain boundary motion may involve more complex phenomena than ordinary solute-boundary interaction and values of n less than 0.5 which vary with the system under consideration and the reaction conditions are possible.

C. Phase Changes

Four different phases are known to exist in the Nb-Al-Ge system at the temperatures investigated, viz.

1.	Ge - rich phase	Nb_5 (Ge, Al)$_3$
2.	Al - rich phase	Nb_2 (Al, Ge)
3.	A - 15 phase	Nb_3 (Al, Ge)
4.	A - 2 phase	(Nb solid solution)

All four phases generally exist in the early stages of a reaction irrespective of the temperature and are disposed as shown in Fig. 8a, which is a scanning electron micrograph of a specimen reacted at 1700°C for 5 seconds. The Ge-rich phase forms the innermost layer, surrounded immediately by the Al-rich sigma phase, then the superconducting A-15 phase. All three phases are embedded in the niobium solid solution.

As the reaction proceeds at a given temperature, the Al-rich phase gradually transforms to the A-15 phase and, as Fig. 8b shows, only three phases, the Ge-rich, A-15, and the A-2 phases are left after reacting at 1700°C for 1 minute. At still longer reaction times the Ge-rich phase is also transformed leaving only the A-15 phase in a matrix of niobium

solid solution. The idea of a matrix phase becomes questionable after these times because it was found that on reacting at 1840°C for 15 minutes, the A-15 phase occupies a greater volume of the specimen than does the niobium solid solution. The two phase system is shown in Fig. 8c.

Since the transformation process depends on several variables, the time required for the disappearance of each of these two phases is not specific and for a given temperature may cover a time range. However these time ranges are generally smaller for the higher temperatures than for the lower ones. In addition, the transformations start much sooner at the higher temperatures. For example, no σ-phase was found in a specimen reacted at 1700°C for 5 minutes and no Ge-rich phase at all after reacting at 1700°C for 30 minutes, but all four phases continue to exist after an hour's reaction at 1300°C. Included in Fig. 8 are the EDAX analyses of the various compositions. These qualitative determinations show slight deviations from stoichiometry. This deviation, in the case of the superconducting phase, could explain why the critical temperatures obtained by Pickus et al,[16] were not as good as some of the reported values. The A-15 compositions given in Table IV shows a trend towards stoichiometric composition as the reaction temperature is increased for a given time.

V. CONCLUSIONS AND RECOMMENDATIONS FOR FURTHER WORK

A study of the Nb-Al-Ge system has shown the existence of four phases at the beginning of a reaction, the innermost two layers, the Ge-rich and Al-rich phases, transforming gradually to the A-15 phase as the reaction proceeds. Also for a given reasonable length of time, even though all four phases may exist when a specimen is reacted at 1300°C for this time, only three may remain at a higher temperature, and at an even higher temperature, only the superconducting phase and the niobium solid solutions might by left. This, coupled with the fact that the critical temperature has been found to increase with an increase in reaction temperature,[16] suggests that the presence of either one or both the Ge-rich and Al-rich phases serves to deteriorate the critical temperature at the lower reaction temperatures. However if this were the case then one would have expected an increase in the critical temperature with an increase in the reaction time since those two phases get transformed with time. The contrary was found to be the case by Pickus, et al.[16] who observed higher T_c's for shorter reaction times. Thus the question of high T_c must be basically one of how close the composition of the A-15 phase in the sample is to stoichiometry and this is confirmed by the data on phase identification (Section IVC) which shows that specimens reacted for short times have compositions closer to stoichiometry than those reacted for longer times. In other words high reaction temperatures and short reaction times would be the ideal conditions for the best T_c values in the presence of excess niobium.

It was observed that the A-15 phase thickness increases with time, for a given reaction temperature. This means an increase in the current

0 0 0 0 0 4 7 1 0 1 4 6 8 4

carrying capacity, assuming a constant critical current. In addition, the average grain size was found to increase with time and temperature, the change becoming drastic above 1700°C as a result of of abnormal grain growth. This again confirms the observations of Pickus, et al. on the low values of critical current density at temperatures above 1600°C since the flux lines then lack pinning centers as a result of the coarse grains.

Observations made from the present study and those of others underscore conflicts in the conditions required for optimizing the superconducting properties of the Nb-Al-Ge system. In summary, better T_c values are obtained for short times and high temperatures; better J_c values for low temperatures and short times (assumed to be due to smaller grains) and greater current-carrying capacities for long times. Thus the potential of this system can be fully realized only by compromising on both the reaction time and temperature. However, if a means could be found for pinning the flux lines at high temperatures, then there would not be much to worry about since substantial current-carrying capacities could then be obtained after short reaction times at high temperatures, in addition to the better T_c's.

This work raises a few questions on this system, the most important among them being:

1. How can the flux lines be pinned or how can the grain growth be impeded?
2. What is the best reaction time and temperature for optimum T_c and current-carrying capacity?

3. How do superconducting properties correlate with the A-15 phase composition?

These are areas that could be further studied to bring out the full potential of the Nb-Al-Ge superconducting system.

0 0 0 0 4 7 4 1 6 9 5

ACKNOWLEDGEMENTS

My deepest gratitude goes to Professor M. R. Pickus for his great help during this study. I am highly indebted to Dr. John Ling-Fai Wang for his suggestions which have greatly contributed to the success of this work and also to Messrs. John Holthuis, Lee Johnson and John Jacobsen whose technical assistance helped a great deal.

This work was done under the auspices of the U. S. Energy Research and Development Agency.

REFERENCES

1. S. Foner and B. B. Schwartz, Superconducting Machines and Devices, Plenum Press, (1974).

2. V. L. Newhouse, Editor, Applied Superconductiviity 1-2, Academic Press, (1975).

3. B. T. Matthias, et al., Science 156, 645 (1967).

4. J. R. Gavaler, Applied Phys. Lett. 23, 480 (1973).

5. J. R. Gavaler, et al., J. Appl. Phys. 45, 3009 (1974).

6. Testardi, et al., Solid State Comm. 15, 1 (1974).

7. G. W. Webb, et al., Solid State Comm. 9, 1769 (1971).

8. P. R. Sahm and T. V. Pruss, Phys. Lett. 28A, 707 (1969).

9. S. Foner, et al., Phys. Lett. 38A, 323 (1972).

10. J. Ruzicka, Z. Physik 237, 432 (1970).

11. S. Foner, et al., Phys Lett. 31A, 349 (1970).

12. R. Lohberg, et al., Appl. Phys. Lett. 22, 69 (1973).

13. D. Dew-Hughes, Cryogenics, 435 (August 1975).

14. J. Ruzicka, Cryogenics 14, 434 (1974).

15. A. Muller, J. Less-Common Metals 42, 29 (1975).

16. M. R. Pickus, et al., Appl. Phys. Lett. 29, 810 (1976).

17. K. Hemachalam and M. R. Pickus, J. Less-Common Metals 46, 297 (1976).

18. J. H. Richardson, Optical Microscopy for the Materials Sciences, Marcel Dekker Inc., 599 (1971).

19. Z. Jefferies, Chem. and Met. Eng. 18, 1918.

20. C. J. Simpson, et al., "Grain Boundary Structure and Properties" 201, Academic Press, Editors: G. A. Chadwick and D. A. Smith, (1976).

21. C. J. Simpson, et al., Met. Trans. 2, 987 & 993 (1971).

0 0 0 0 4 7 0 1 6 8 6
0 0 0 0 4 7 1 1 4 7 8

TABLES

Table I Materials used.

Material	Source	Purity	Form
Nb	Wah Chang Albany Corporation	99.9	Powder (-270 + 400 mesh)
Al	United Mineral and Chemical	99.999	Rod
Ge	Orion Chemical Co.	99.999	Random Pieces

Table II Readings (Overall average values)

	Phase Thickness (microns)				Grain Size (microns)		
Time (sec)	1300°C	1500°C	1700°C	1840°C	1500°C	1700°C	1840°C
10			1.62	1.87			
20			1.92	2.51		3.10	7.45
60		1.90	2.63	3.59		5.51	11.18
180						6.64	16.26
300		3.73	5.38	8.35	4.87	8.79	28.48
600		4.68			6.09		
900	3.02	5.16	6.79		6.63	12.66	41.00
1200		5.95			7.73		
1800	4.27	6.35			8.73	16.06	
3600	5.20						
7200	7.68						

Table III Slopes and Correlation for Figs. 6b and 7c.

Temperature	Phase Thickness Slope (n)	Phase Thickness Correlation (r^2)	Grain Size Slope (n)	Grain Size Correlation (r^2)
1300°C	0.42	0.96		
1500°C	0.36	0.99	0.33	-0.99
1700°C	0.34	-0.99	0.35	0.99
1840°C	0.44	-0.99	0.46	-0.97

Table IV Changes in A-15 Composition (Atomic %) with Time and Temperature of Reaction (Determined by EDAX)

	Readings taken at 1700°C for 5 sec.	
Element	Analysis No. 1	Analysis No. 2
Nb	61.7	70.0
Al	34.5	26.8
Ge	3.8	3.2

	Readings taken at 1700°C for 1 min.		
Element	Analysis No. 1	Analysis No. 2	Analysis No. 3
Nb	61.6	58.5	59.2
Al	25.2	26.2	31.9
Ge	13.2	15.3	8.9

	Readings taken at 1700°C for 15 min.			
Element	Analysis No. 1	Analysis No. 2	Analysis No. 3	Analysis No. 4
Nb	63.6	62.4	62.3	62.2
Al	23.0	23.5	23.1	24.2
Ge	13.4	14.1	14.6	13.6

	Readings taken at 1500°C for 15 min.	
Element	Analysis No. 1	Analysis No. 2
Nb	63.4	64.9
Al	26.1	23.8
Ge	10.5	11.3

	Readings taken at 1840°C for 15 min.			
Element	Analysis No. 1	Analysis No. 2	Analysis No. 3	Analysis No. 4
Nb	64.8	64.0	60.4	61.8
Al	26.7	27.3	26.7	27.0
Ge	8.5	8.7	12.9	11.2

FIGURE CAPTIONS

Fig. 1. Structure of the A-15 phase.

Fig. 2. Optical Micrographs showing changes in the microstructure of the Nb-Al-Ge system with time and temperature: (a) 1500°C for 1 min. (b) 1700°C for 1 min. (c) 1840°C for 1 min. (d) 1500°C for 5 min. (e) 1700°C for 5 min. (f) 1840°C for 5 min.

Fig. 3. Abar furnace. 1. Extension tube, 2. Tantalum rod, 3. back filling port, 4. electrical leads, 5. tungsten mesh heating element, 6. Nb specimen, 7. radiation shields, 8. water cooled wall, 9. W-5% Re vs. W-26% Re thermocouple point, 10. vacuum connection, 11. quartz tube, 12. smaller quartz tube containing Al-Ge eutectic, 13. graphite crucible, 14. electric heater.

Fig. 4. Microstructure of the Al-Ge eutectic.

Fig. 5. Sintered Nb compact infiltrated with Al-Ge eutectic.

Fig. 6. Variation of the A-15 phase thickness with time. (a) linear scale, (b) log-log plot.

Fig. 7. Grain growth in the A-15 phase. (a) average grain size - time plots (isothermal plots), (b) average grain size - temperature plot (isochronal plots), (c) log-log plot of 7a.

Fig. 8. Scanning electron micrograph showing microstructural changes with reaction. (a) specimen reacted at 1700°C for 5 seconds, (b) specimen reacted at 1700°C for 1 minute, (c) specimen reacted at 1700°C for 15 minutes.

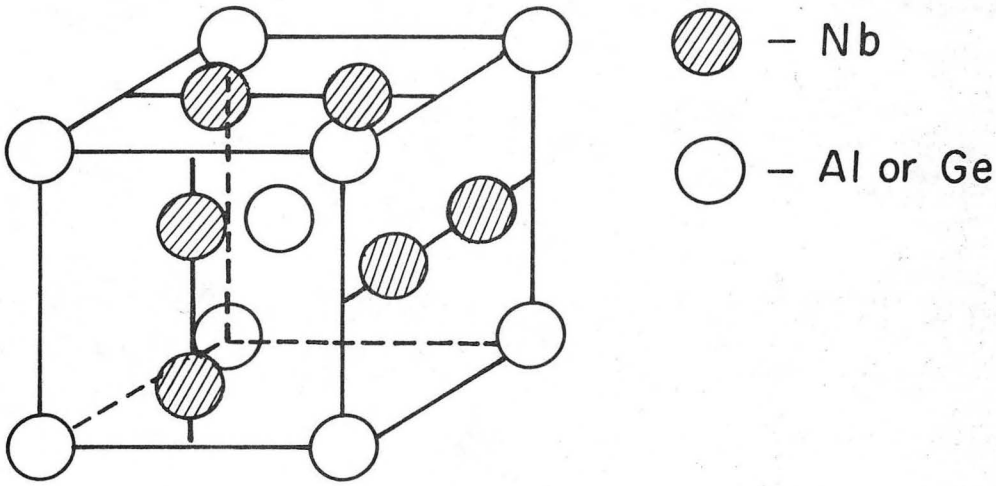

XBL774-865

Fig. 1

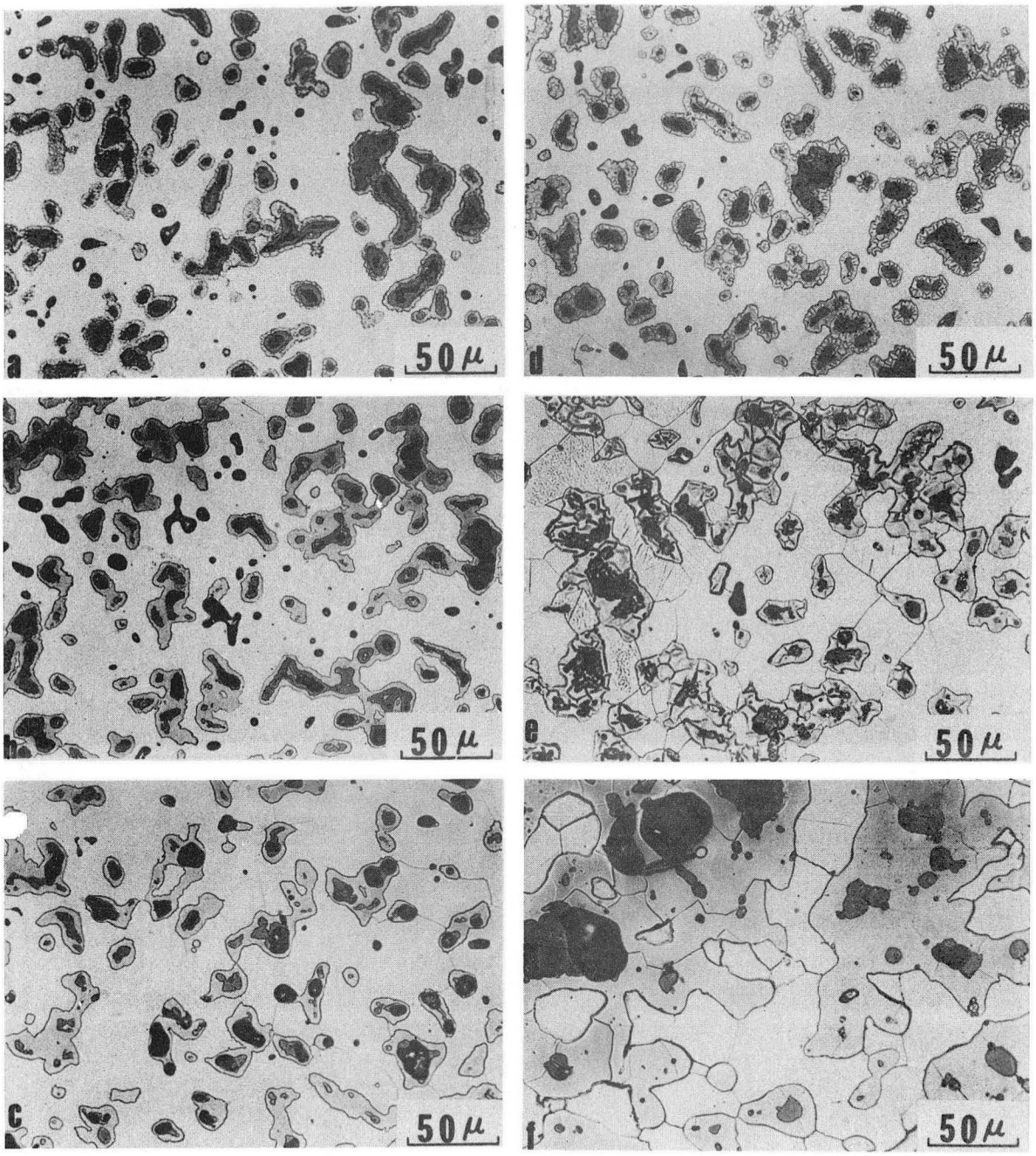

XBB 774-4220

Fig. 2

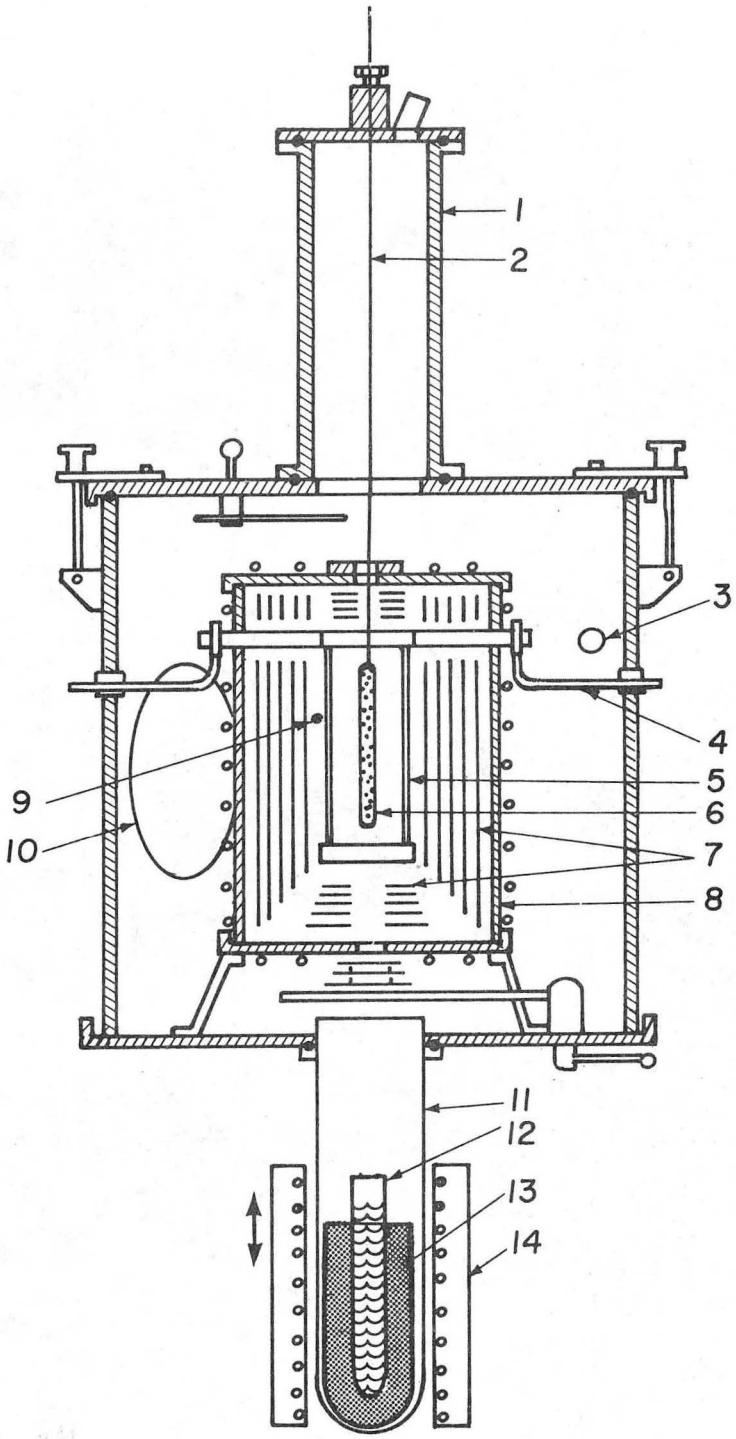

XBL774-864

Fig. 3

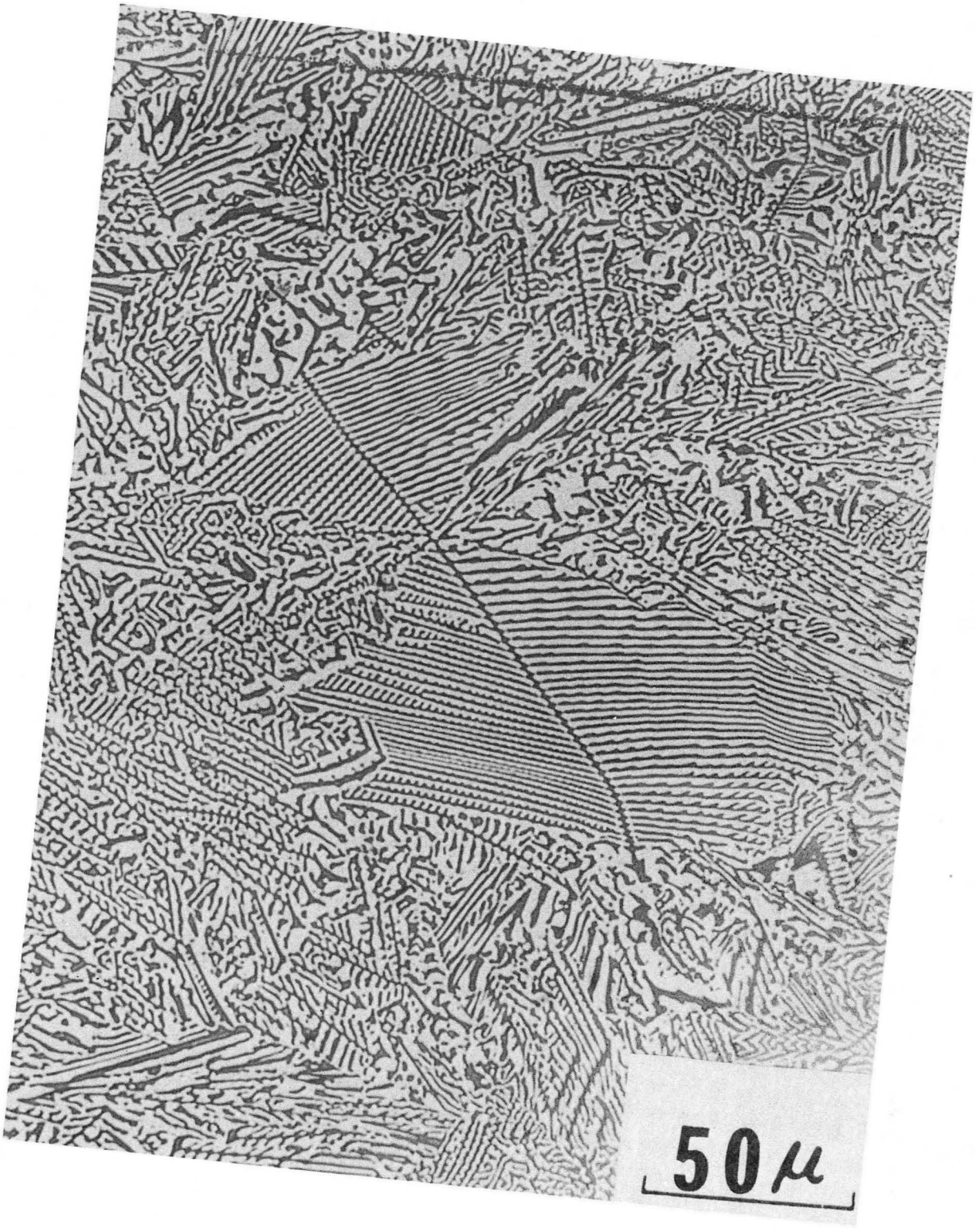

XBB 773-1537A

Fig. 4

0 0 0 0 4 7 7 P 4 8 P 8

XBB 774-1538A

Fig. 5

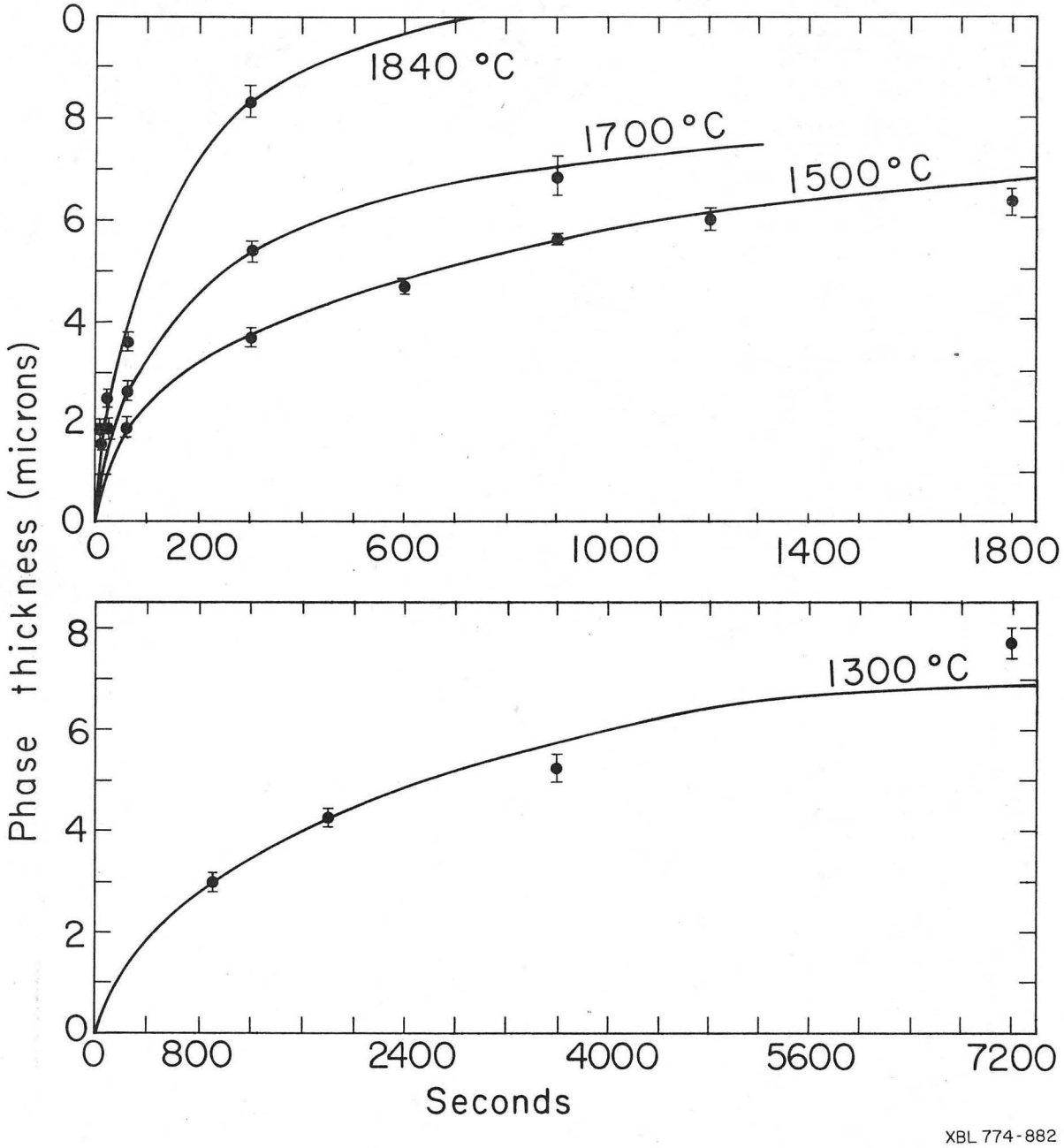
1840 °C
1700 °C
1500 °C
1300 °C
Phase thickness (microns)
Seconds
0
2
4
6
8
0
200
600
1000
1400
1800
0
800
2400
4000
5600
7200
XBL 774-882

Fig. 6a

0 0 0 0 4 7 1 1 4 8 2

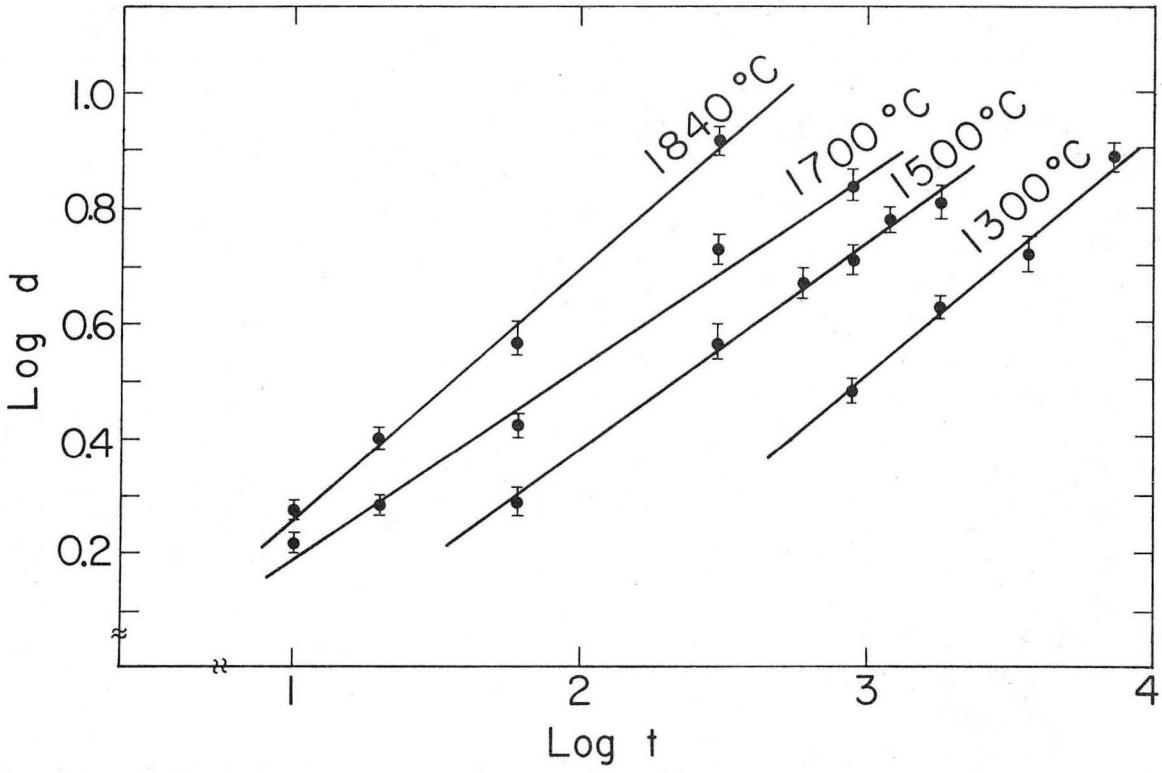

XBL774-866

Fig. 6b

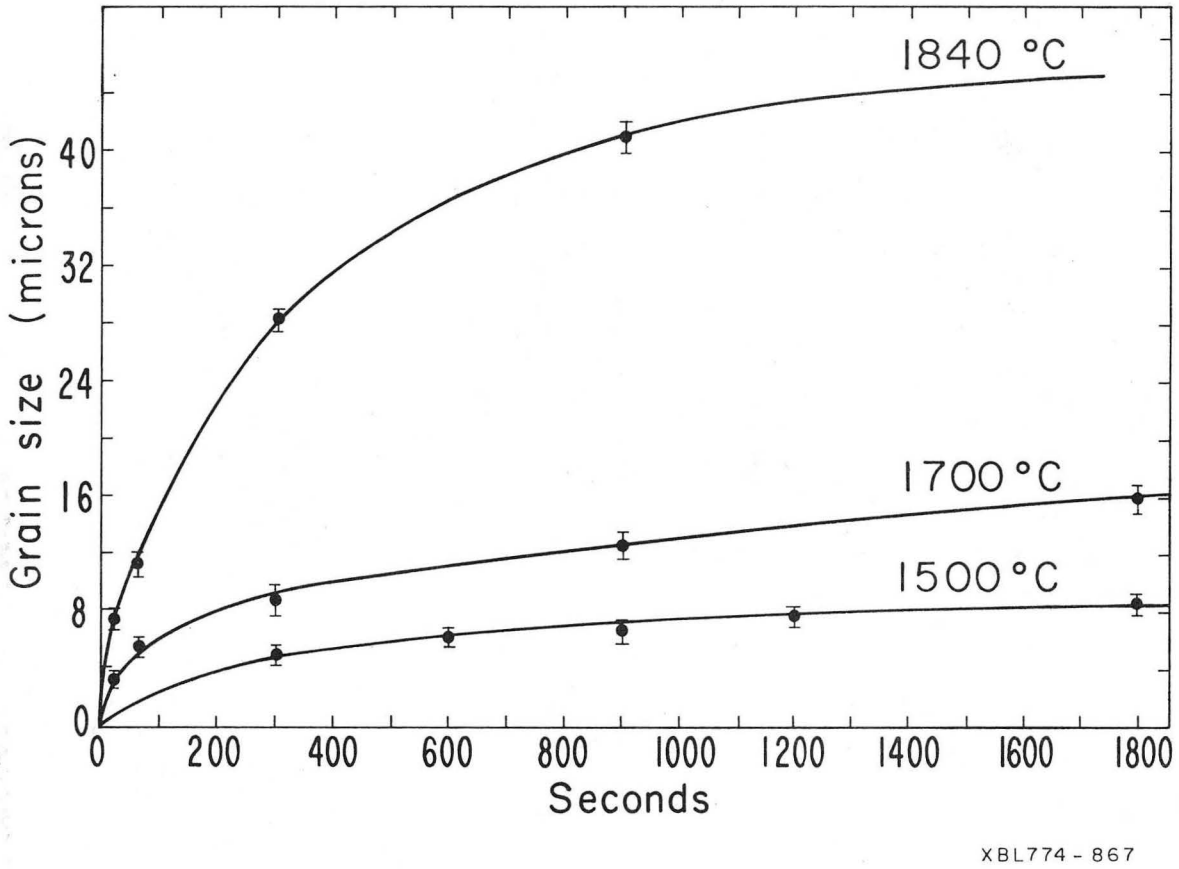
1840 °C
1700 °C
1500 °C
Grain size (microns)
0
8
16
24
32
40
0
200
400
600
800
1000
1200
1400
1600
1800
Seconds
XBL774-867

Fig. 7a

0 0 0 0 4 7 7 9 4 6 8 9

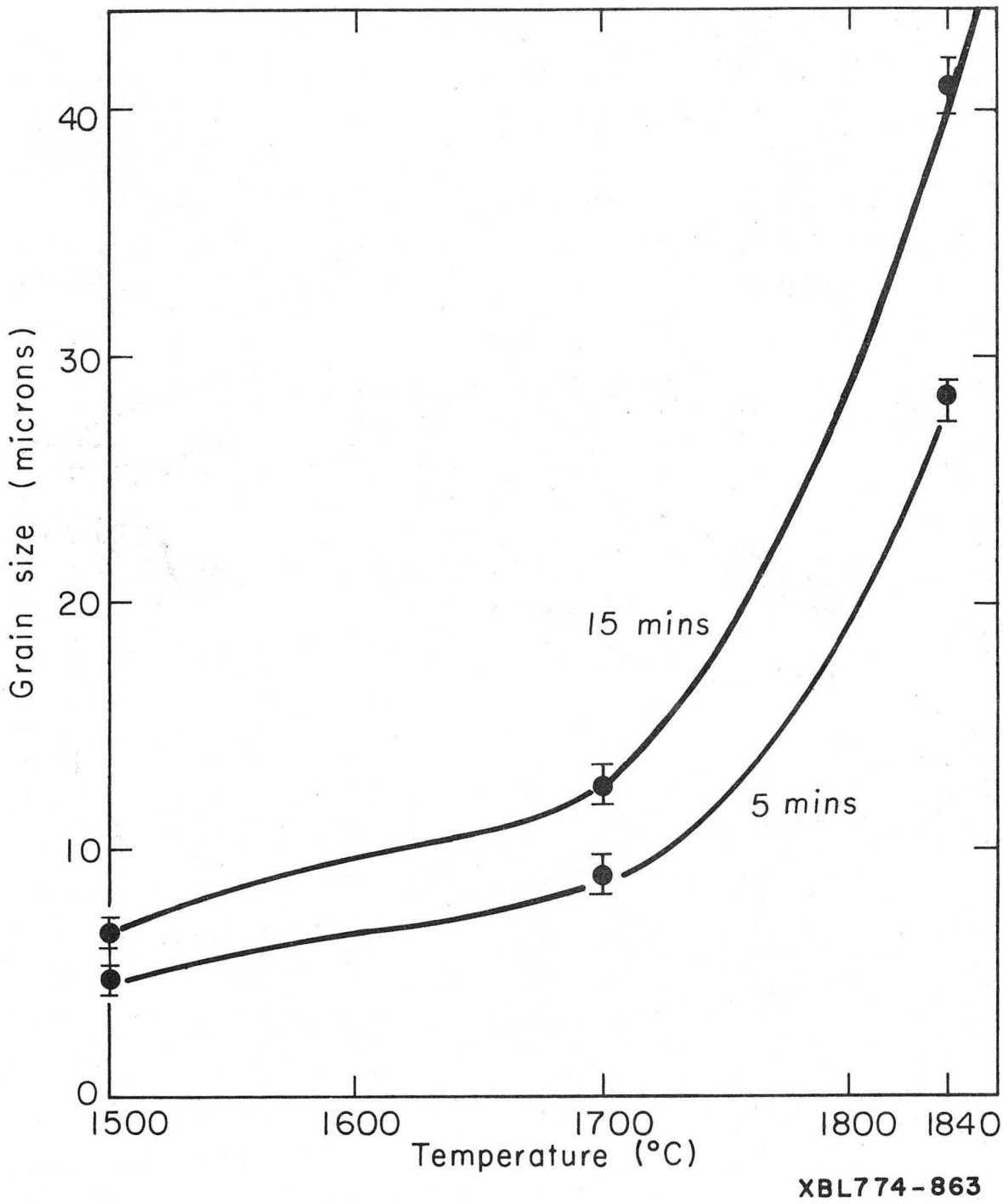

Fig. 7b

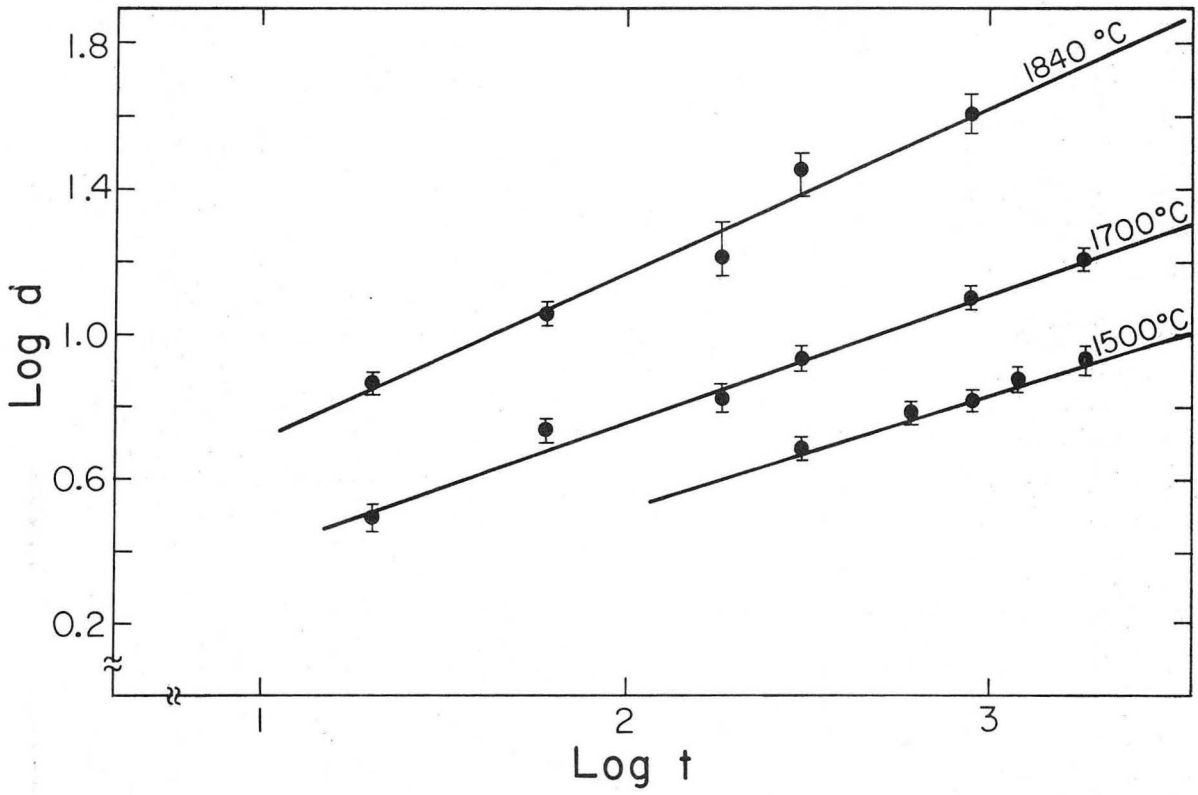

XBL774-862

Fig. 7c

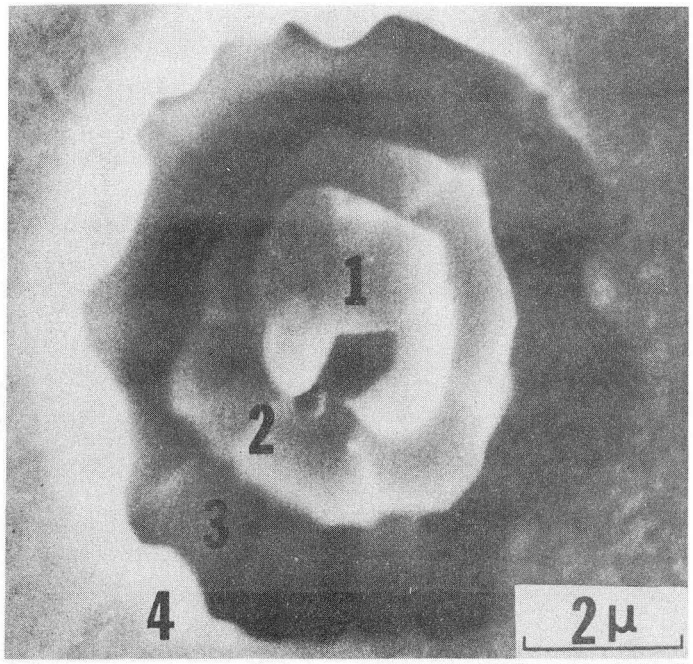

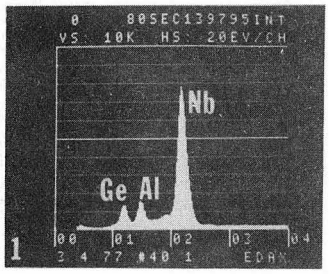

Ge-rich Phase
Nb: 39.8%
Al: 32.3%
Ge: 27.9%

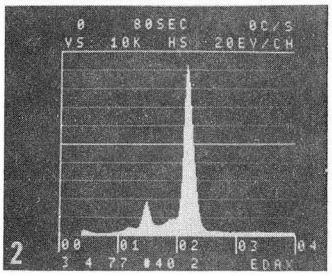

Al-rich Phase
Nb: 50.2%
Al: 43.0%
Ge: 6.8%

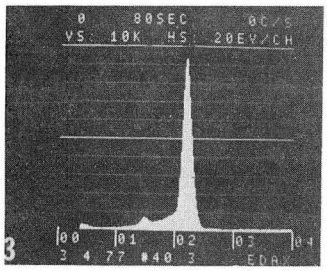

A-15 Phase
Nb: 70.0%
Al: 26.8%
Ge: 3.2%

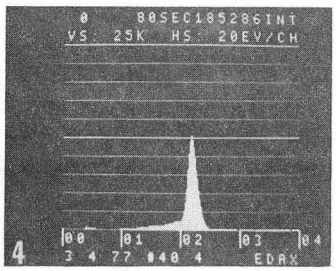

A-2 Phase
Nb: 95.1%
Al: 4.5%
Ge: 0.4%

XBB 774-4173

Fig. 8a

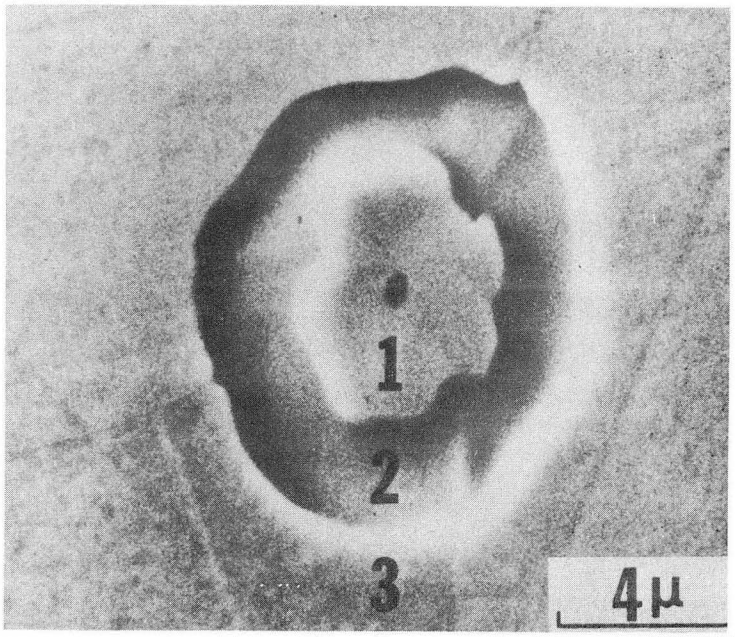

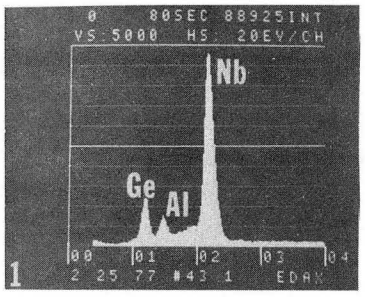

Ge-rich Phase
Nb: 41.6%
Al: 31.1%
Ge: 27.3%

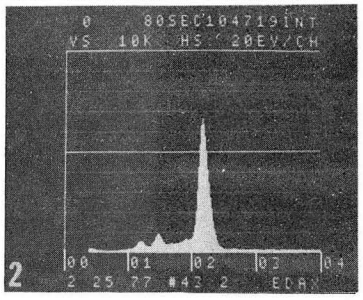

A-15 Phase
Nb: 61.6%
Al: 25.2%
Ge: 13.2%

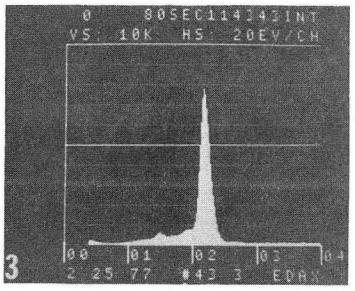

A-2 Phase
Nb: 86.2%
Al: 10.8%
Ge: 3.0%

XBB 774-4172

Fig. 8b

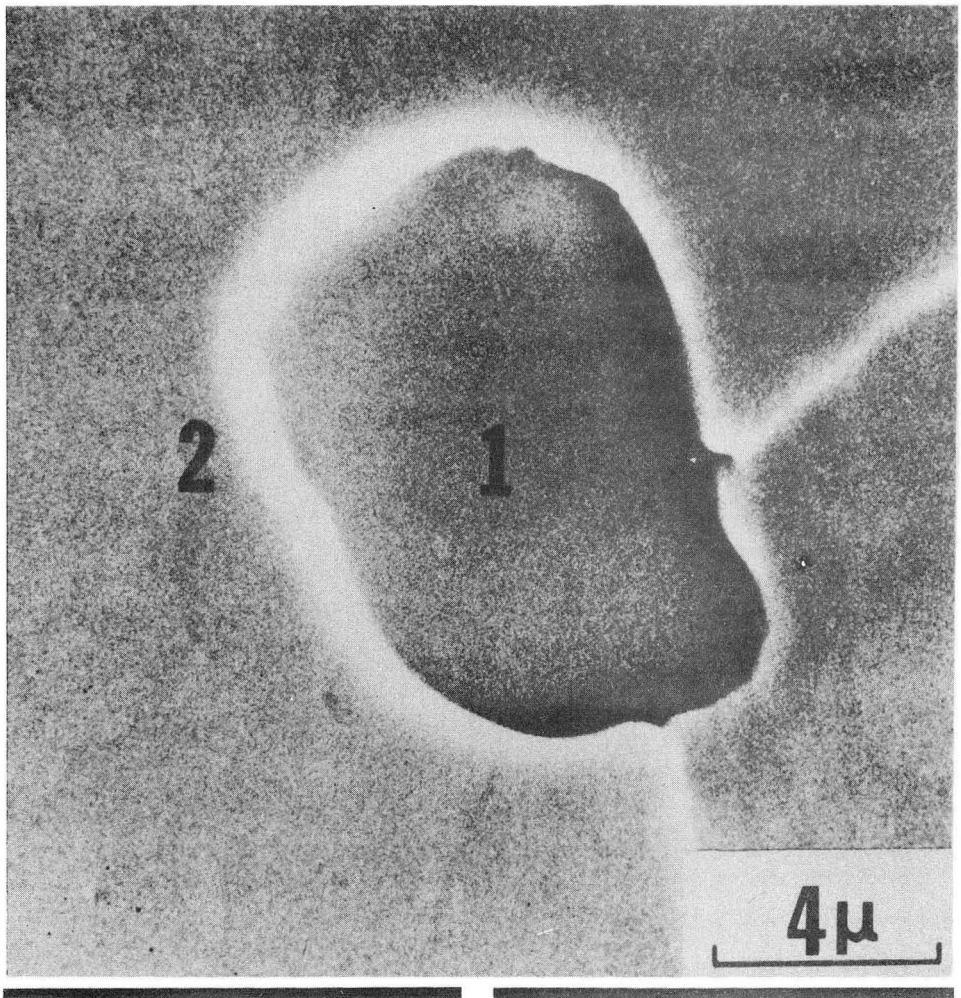

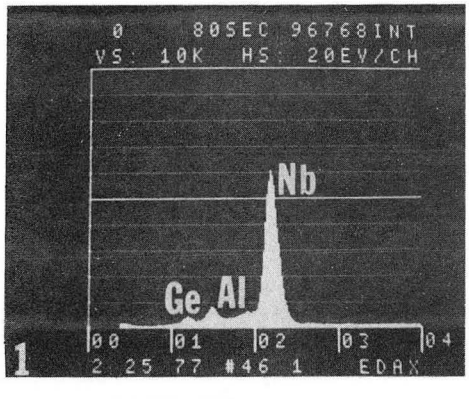

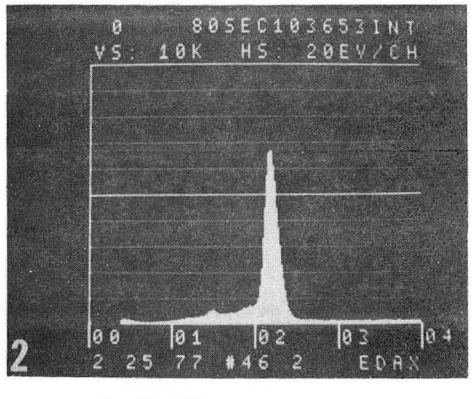

A-15 Phase
Nb: 63.6%
Al: 23.0%
Ge: 13.4%

A-2 Phase
Nb: 86.7%
Al: 10.7%
Ge: 2.6%

XBB 774-4171

Fig. 8c

0 0 0 0 8 7 7 9 4 6 8 2

This report was done with support from the United States Energy Research and Development Administration. Any conclusions or opinions expressed in this report represent solely those of the author(s) and not necessarily those of The Regents of the University of California, the Lawrence Berkeley Laboratory or the United States Energy Research and Development Administration.

TECHNICAL INFORMATION DIVISION
LAWRENCE BERKELEY LABORATORY
UNIVERSITY OF CALIFORNIA
BERKELEY, CALIFORNIA 94720